Electronic Supplementary Material (ESI) for Nanoscale.
This journal is © The Royal Society of Chemistry 2024

Electronic Supplementary Information

Polyoxometalate-mediated syntheses of three structurally new silver clusters

Jing Zhang, Yuanyuan Dong, Lan Deng, Manzhou Chi, Yeqin Feng, Mengyun Zhao, Hongjin Lv*, and Guo-Yu Yang

MOE Key Laboratory of Cluster Science, Beijing Key Laboratory of Photoelectric/Electrophotonic Conversion Materials, School of Chemistry and Chemical Engineering, Beijing Institute of Technology, Beijing 102488, P. R. China

Corresponding author. E-mail: hlv@bit.edu.cn

Table of contents

Experimental Section

Chemicals and Materials. The $(^{i}PrSAg)_n$ precursor and the $TBA_4H_6[\alpha\text{-}SiW_9O_{34}]$ were synthesized according to previously reported procedures.[1, 2] The chemicals and solvents used in the syntheses were purchased from commercial sources and used as received without further purification. ^{i}PrSH (Adamas-beta®) was purchased from Shanghai Titan Scientific Co.,Ltd and used as received. Silver acetate (CH_3COOAg) was purchased from Shanghai Macklin Biochemical Co., Ltd and used as received. Silver nitrate ($AgNO_3$) was purchased from Sinopharm Chemical Reagent Co., Ltd and used as received.

Characterization. The FT-IR spectra were performed on a Bruker Tensor II spectrometer using ~2 wt% KBr pellets in the range of 4000 ~ 400 cm^{-1}. The UV-Vis spectra were acquired on a Techcomp UV 2600 spectrophotometer at room temperature in the 200 ~ 800 nm range. Single-crystal X-ray crystallography was carried out on a Bruker D8 Venture diffractometer operated at 40 kV and 40 mA with Mo Kα radiation (λ = 0.71073 Å). The X-ray Photoelectron Spectrum (XPS) was measured on a PHI5000 Versaprobe III. The steady-state luminescence quenching spectra was measured using Edinburgh Instruments FS5 Spectrofluorometer. Emission lifetime was measured with an EPL-365 picosecond pulsed diode laser system (pulse output 365 nm). The XPS data were carried out on a PHI 5000 Versaprobe III instrument. The Scanning electron microscopy (SEM)/EDS measurements were carried out on a ZEISS supra55. Powder X-ray diffraction (PXRD) analyses were measured on a MiniFlex 600 diffractometer with a Cu-Kα X-ray radiation source. The photoluminescence performance of three crystal powders was tested using Edinburgh Instruments spectrofluorometer FLS1000. Photothermal measurements were conducted using Laser MGL-III-532nm-300mW. The photothermal behavior of the sample was monitored by thermal imaging camera (Fotric 326C). Infrared photos and real-time temperatures were extracted from the video by FLIR tools software.

Synthesis of ^{i}PrSAg. Silver nitrate ($AgNO_3$) was added to 75 ml of acetonitrile and dissolved by ultrasonication, 2.8 ml of isopropyl mercaptan and 5 ml of triethylamine were dissolved in 100 ml of ethanol solution, mixed and stirred for 3 hours at room temperature in darkness, filtered and separated

to obtain a yellow powder of silver isopropyl mercaptan, washed with 10 ml of ethanol and 20 ml of ethyl ether, and dried in vacuum (yield 97%).

Synthesis of $[(SiW_9O_{34})@Ag_{24}(^iPrS)_{11}(DPPP)_6Cl]_2(SiW_{12}O_{40})$ (Ag_{24}). AgOAc (0.1 mmol, 16.7 mg) and $TBA_4H_6[SiW_9O_{34}]$ (100 mg) were added in a mixture of acetonitrile (3 mL) and deionized water (50 μL), After stirring for two hours at room temperature, ^{i}PrSAg (0.109 mmol, 20 mg), 1,3-Bis(diphenylphosphino)propane (0.073 mmol, 30 mg), acetonitrile (2 ml) and *N*,*N*-dimethylformamide (1 mL) were added in turn. Then the mixed reactants were transferred to a 25 mL Teflon bottles and tightly sealed in stainless steel autoclaves. The solvothermal procedure was carried out on a temperature-controlled electric oven at 60 °C for 48 h. When the solution cooled to room temperature, the orange crystals of **Ag_{24}** were obtained immediately with a yield of 0.03 g (34.7%, based on Ag).

Synthesis of $[(SiW_9O_{34})@Ag_{22}Cu(^iPrS)_{11}(DPPP)_6Cl](SbF_6)_2$ ($Ag_{22}Cu$). Synthesis of **$Ag_{22}Cu$** was the same as that of **Ag_{24}**, except adding some extra copper acetylacetonate (15 mg, 0.057 mmol) and sodium hexafluoroantimonate (10 mg, 0.039 mmol) in the last step. Orange block crystals **$Ag_{22}Cu$** were isolated after 1 month in ~17.9% yield (0.014 g, based on Ag).

Synthesis of $\{Ag_{16}(^iPrS)_6(DPPP)_8(CH_3COO)_4[Co_4(OH)_3SiW_9O_{33}]_2\}(CH_3CN)_4(H_2O)_2$ ($Ag_{16}Co_8$). Synthesis of **$Ag_{16}Co_8$** was similar to **Ag_{24}** cluster, except cobalt acetylacetonate (60 mg, 0.233 mmol) was additional in the last step. Red block crystals **$Ag_{16}Co_8$** were obtained immediately with a yield of 0.029 g (20.6%, based on Ag) when the solution cooled to room temperature.

Single-Crystal X-ray Crystallography

The crystals of **Ag_{24}**, **$Ag_{22}Cu$** and **$Ag_{16}Co_8$** with appropriate dimensions were selected under an optical microscope and quickly immersed in crystal oil to prevent decomposition at both ends for data collection at 180 K. Crystallographic data were collected on a Bruker SMART APEX II CCD diffractometer with Mo Kα radiation (graphite monochromator, λ = 0.71073 Å). Data collection, indexing, and initial cell refinements were all performed using APEX II software. Frame integration

and final cell refinements were done using SAINT software based on optimal reflections. By using the Superflip structure solving program, Olex2 was used to solve the structure by charge flipping, and ShelXL was used to optimize the structure by least-squares. All non-H atoms of the complexes were refined with anisotropic thermal parameters. Hydrogen atoms in **Ag_{24}** and **$Ag_{22}Cu$** were included in idealized positions and refined in a fixed geometry with respect to their carrier atoms. Crystal structure graphics and their packing diagrams were carried out by using Diamond 4 software. CCDC 2312087, 2343569 and 2336489 contain the supplementary crystallographic data for **Ag_{24}**, **$Ag_{22}Cu$** and **$Ag_{16}Co_8$**, respectively. The crystallographic data can be obtained from The Cambridge Crystallographic Data Centre via www.ccdc.cam.ac.uk/data_request/cif.

Bond valence sum (BVS) calculation

The BVS values were calculated by the expression for the variation of the length r_{ab} of a bond between two atoms a and b in observed crystal with valence V_a.[3]

$$V_a = \sum exp(\frac{r_0 - r_{ab}}{B})$$

where B is constant equal to 0.37 Å, r_0 is bond valence parameter for a given atom pair.

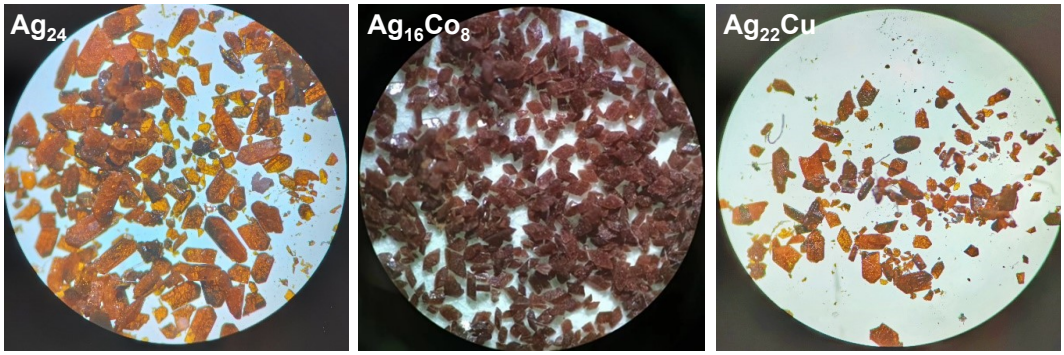

Fig. S1 The digital photographs of **Ag_{24}**, **$Ag_{16}Co_8$** and **$Ag_{22}Cu$** crystals taken under the microscope.

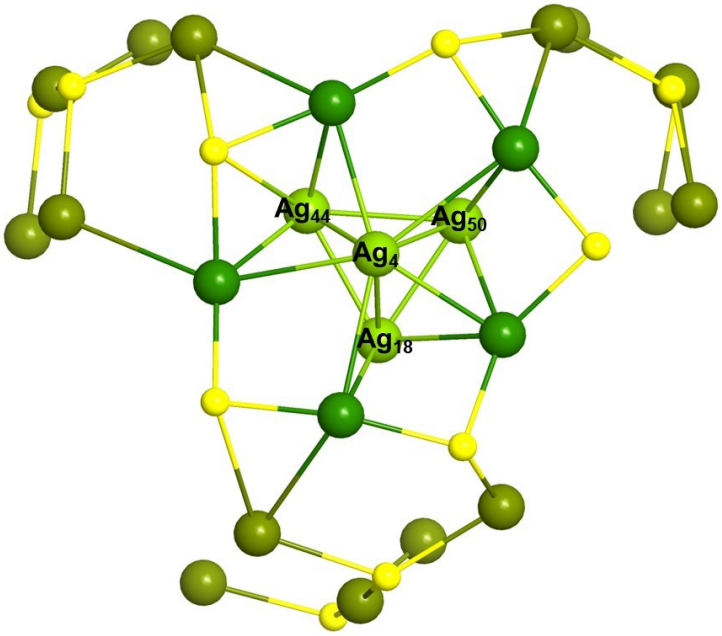

Fig. S2 Three different coordination modes of Ag atoms in **Ag_{24}**.

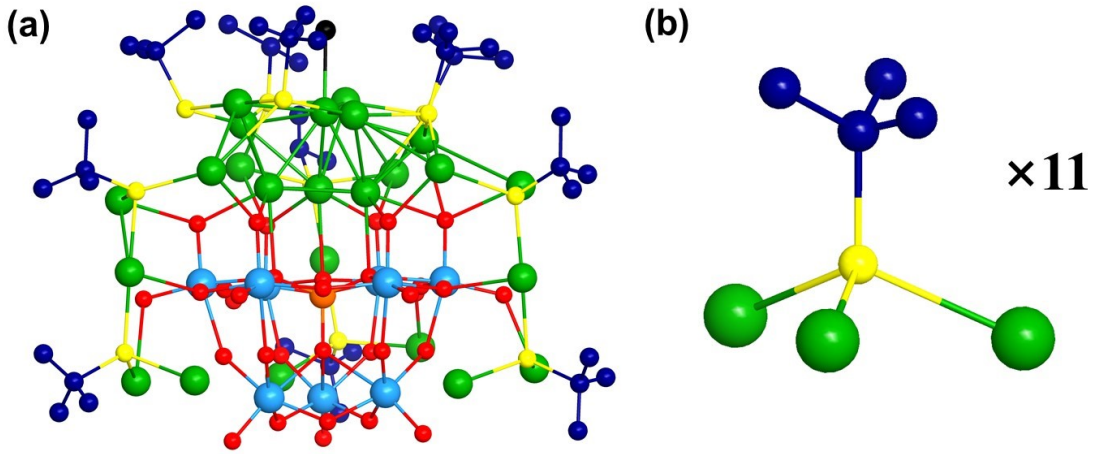

Fig. S3 The coordination modes of 11 $^{i}PrS^{-}$ ligands towards Ag atoms in **Ag_{24}** cluster. Color codes: green, Ag; yellow, S; red, O; blue, W; orange, Si; black, Cl; dark blue, C.

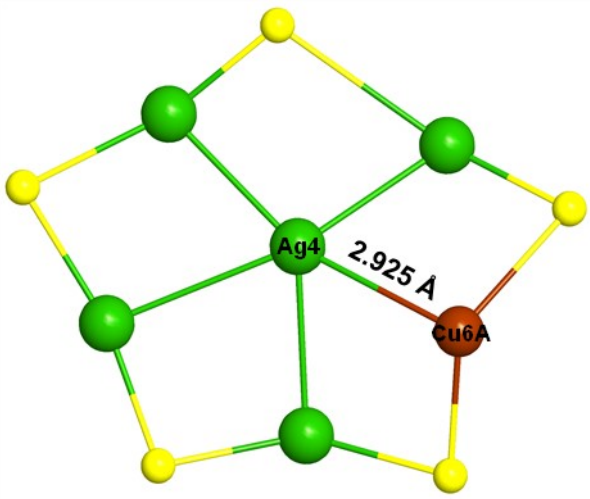

Fig. S4 The Ag_5CuS_5 unit in $Ag_{22}Cu$ cluster. Color codes: green, Ag; yellow, S; brown, Cu.

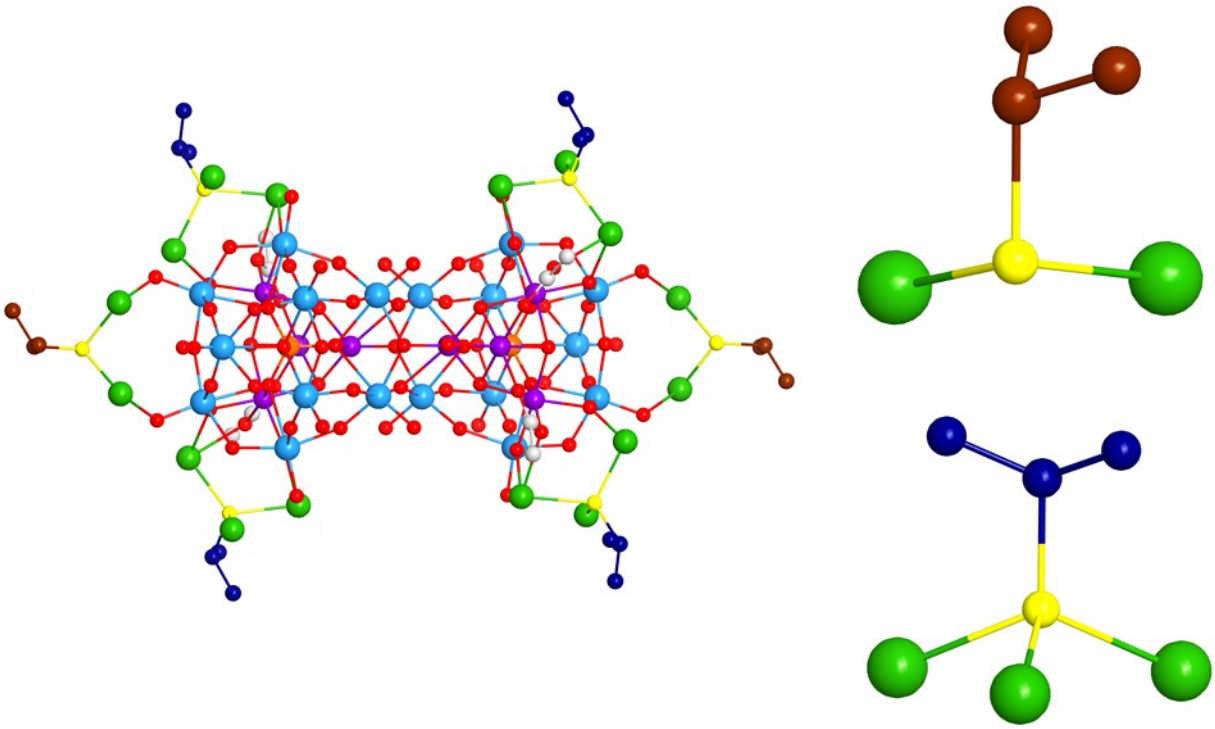

Fig. S5 The coordination modes of 6 $^{i}PrS^{-}$ ligands towards Ag atoms in $Ag_{16}Co_8$ cluster. Color codes: green, Ag; blue, W; orange, Si; yellow, S; red, O; brown, Cu; gray, C; purple, Co; brown, C; dark blue, C; white, C.

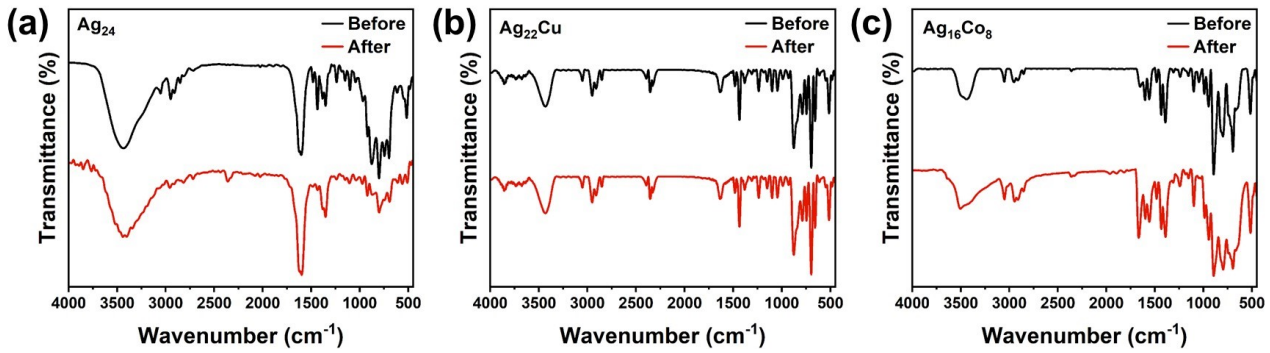

Fig. S6 FT-IR spectra of (a) **Ag_{24}**, (b) **$Ag_{22}Cu$** and (c) **$Ag_{16}Co_8$** clusters before and after photothermal tests.

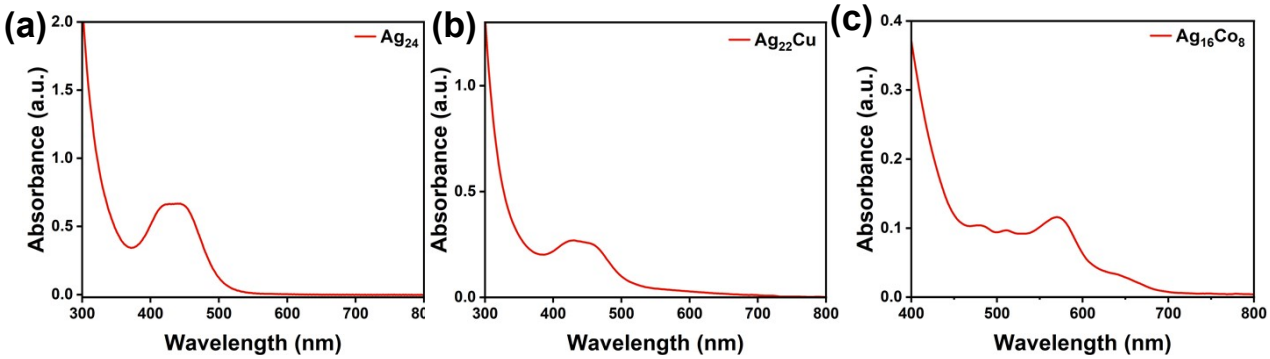

Fig. S7 The UV-vis absorption spectra of (a) **Ag_{24}** and (b) **$Ag_{22}Cu$** dissolved in DMF and (c) **$Ag_{16}Co_8$** dissolved in DMSO at room temperature.

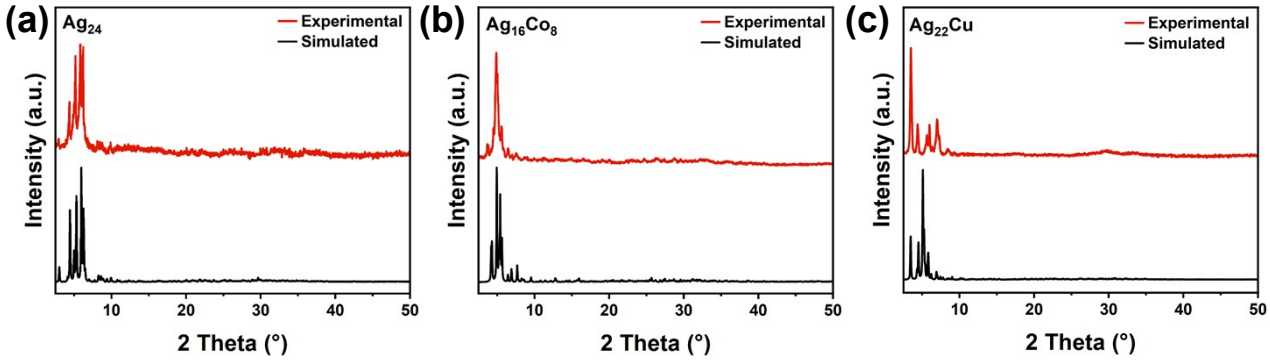

Fig. S8 Experimental and simulated PXRD patterns of (a) Ag_{24}, (b) $Ag_{22}Cu$ and (c) $Ag_{16}Co_8$ clusters.

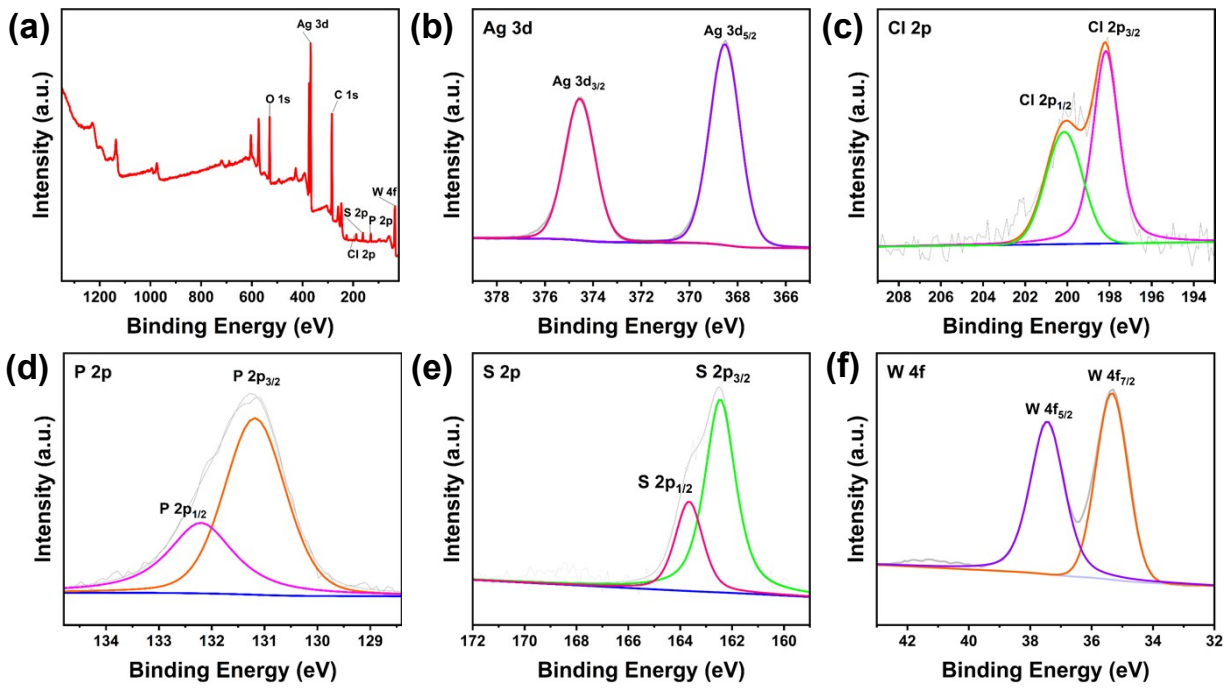

Fig. S9 (a) XPS survey spectrum of **Ag_{24}** cluster; high resolution XPS spectra of (b) Ag 3d, (c) Cl 2p, (d) P 2p, (e) S 2p and (f) W 4f in **Ag_{24}** cluster.

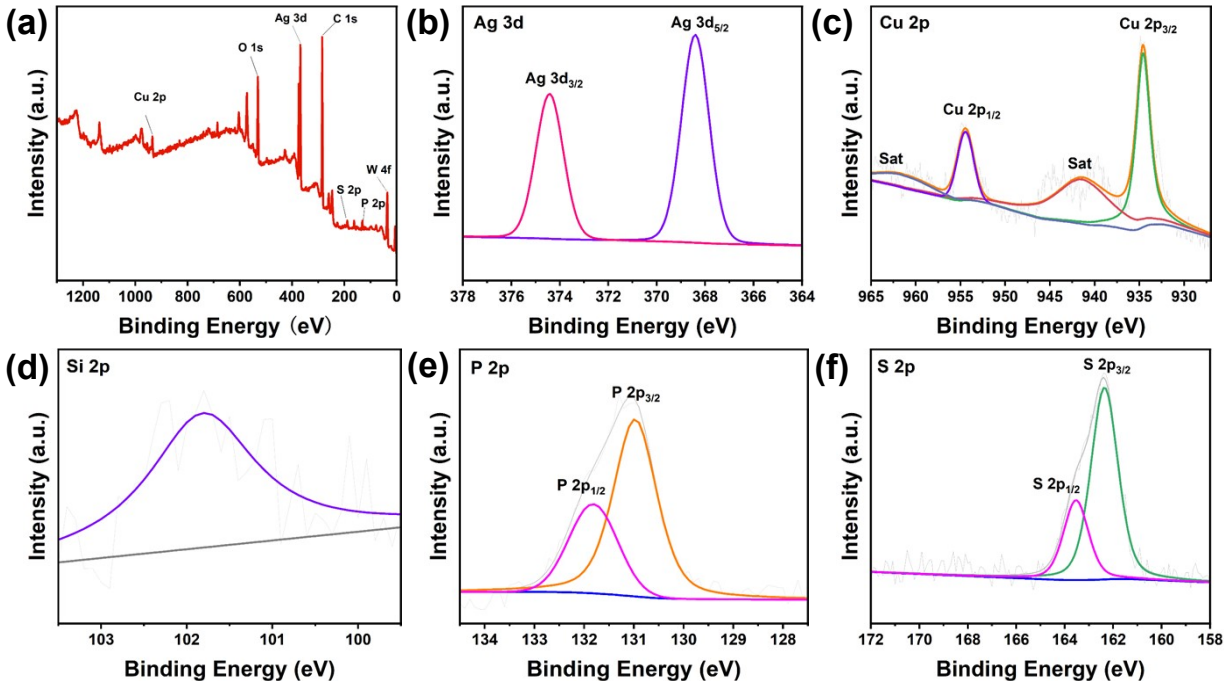

Fig. S10 (a) XPS survey spectrum of **$Ag_{22}Cu$** cluster; high resolution XPS spectra of (b) Ag 3d, (c) Cl 2p, (d) P 2p, (e) S 2p and (f) W 4f in **$Ag_{22}Cu$** cluster.

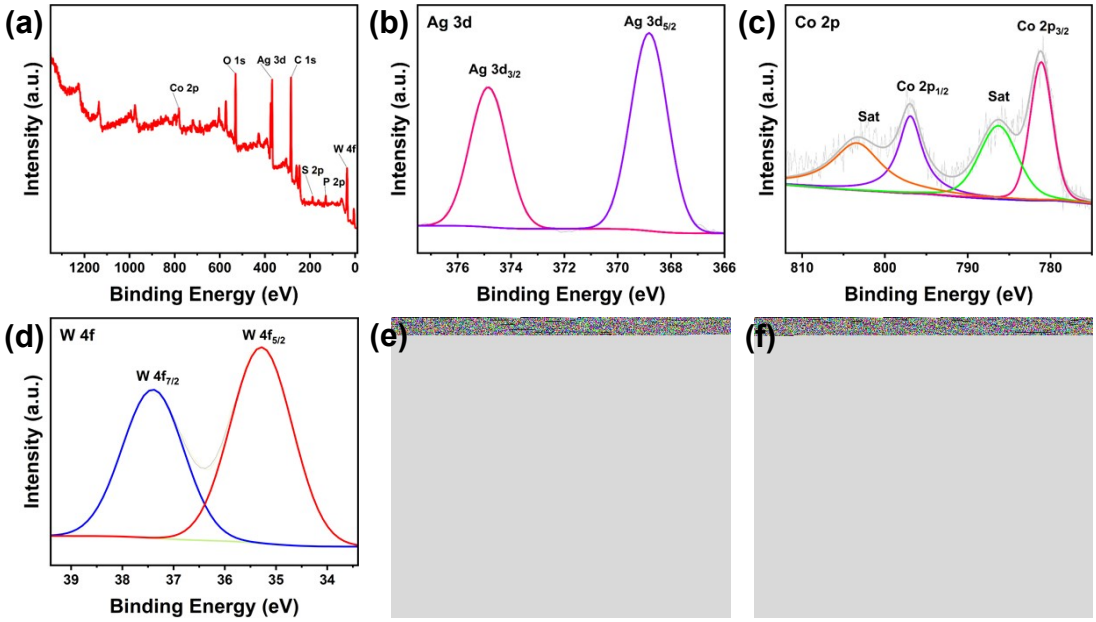

Fig. S11 (a) XPS survey spectrum of $\mathbf{Ag_{16}Co_8}$ cluster; high resolution XPS spectra of (b) Ag 3d, (c) Cl 2p, (d) P 2p, (e) S 2p and (f) W 4f in $\mathbf{Ag_{16}Co_8}$ cluster.

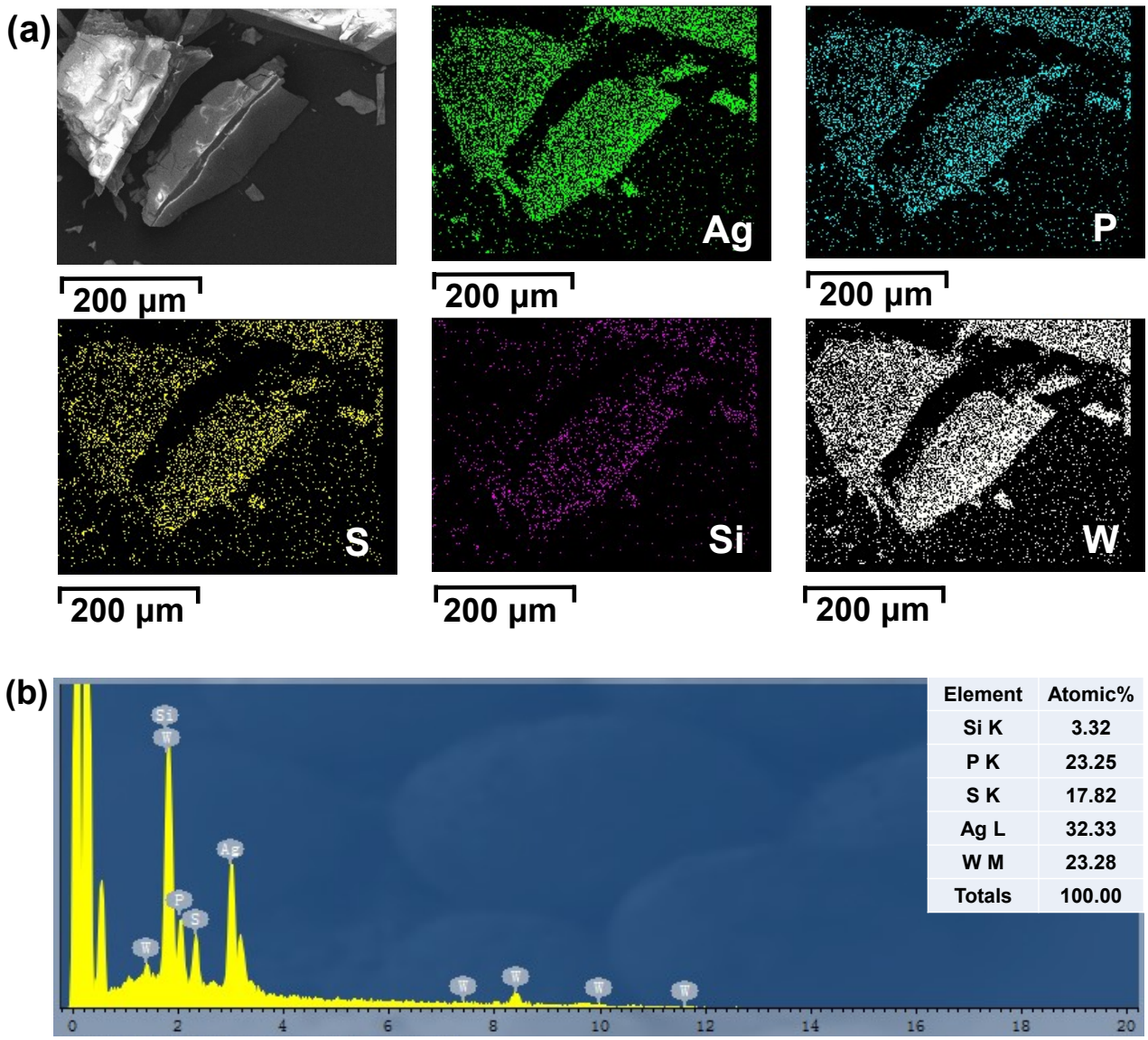

Fig. S12 (a) SEM and elemental mapping images, and (b) EDS result of $\mathbf{Ag_{24}}$.

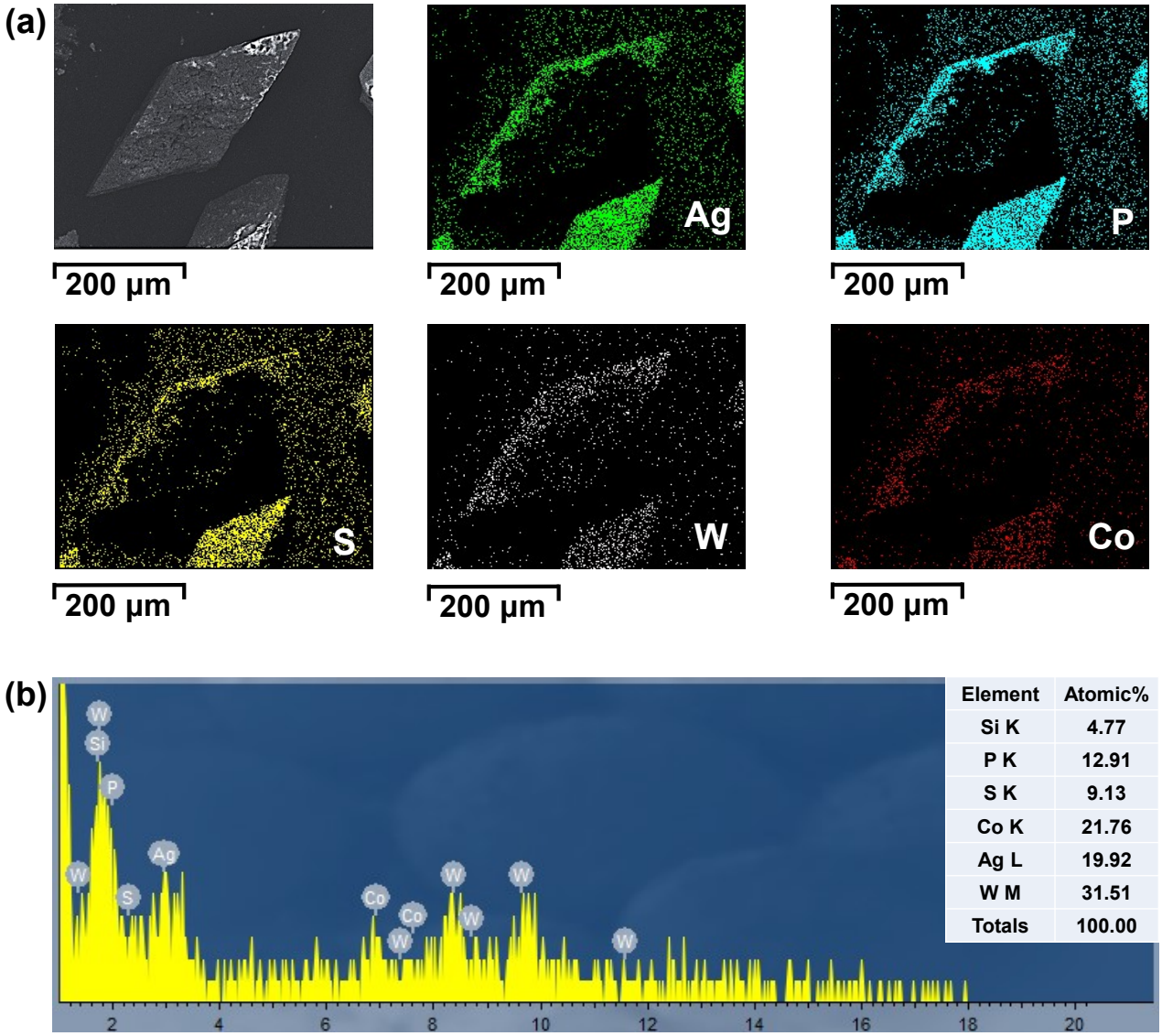

Fig. S13 (a) SEM and elemental mapping images, and (b) EDS result of $Ag_{16}Co_8$.

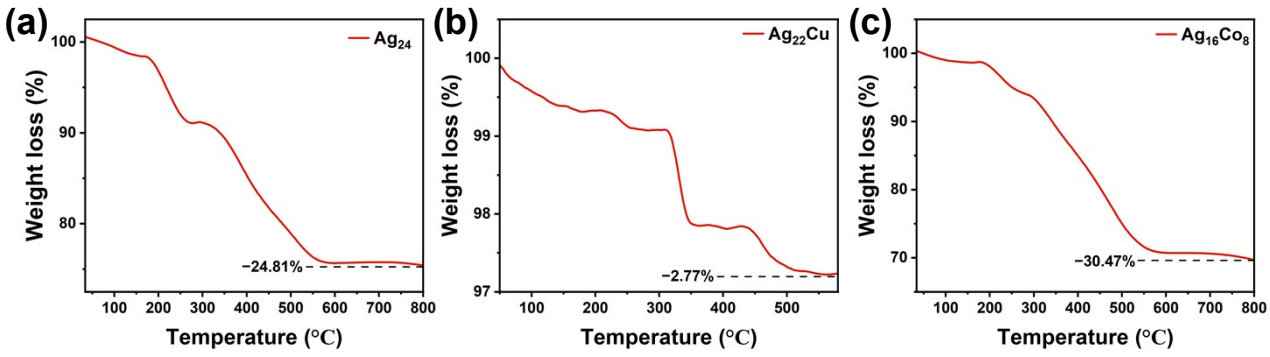

Fig. S14 TGA curves of (a) Ag_{24}, (b) $Ag_{22}Cu$ and (c) $Ag_{16}Co_8$ at a scanning rate of 10 °C/min under air atmosphere.

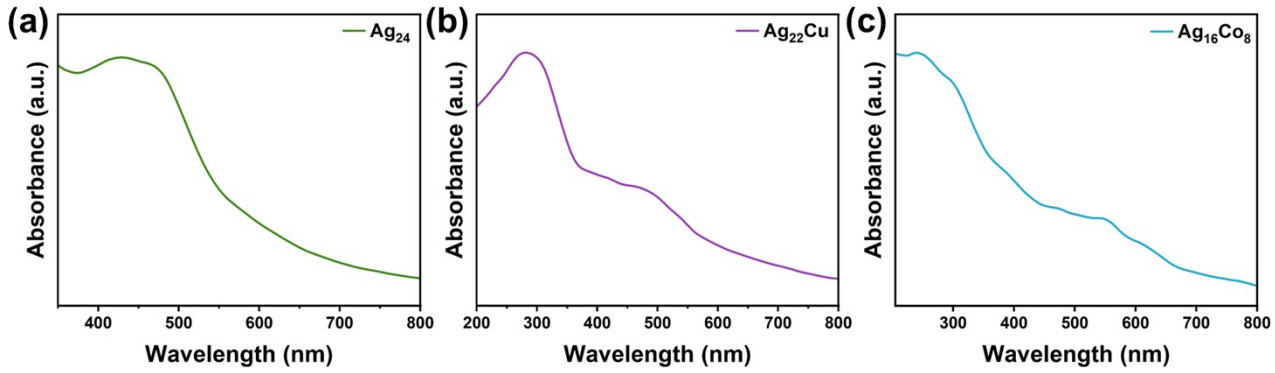

Fig. S15 The solid-state UV−vis spectra of **(a) Ag_{24}, (b) $Ag_{22}Cu$ and (c) $Ag_{16}Co_8$** clusters.

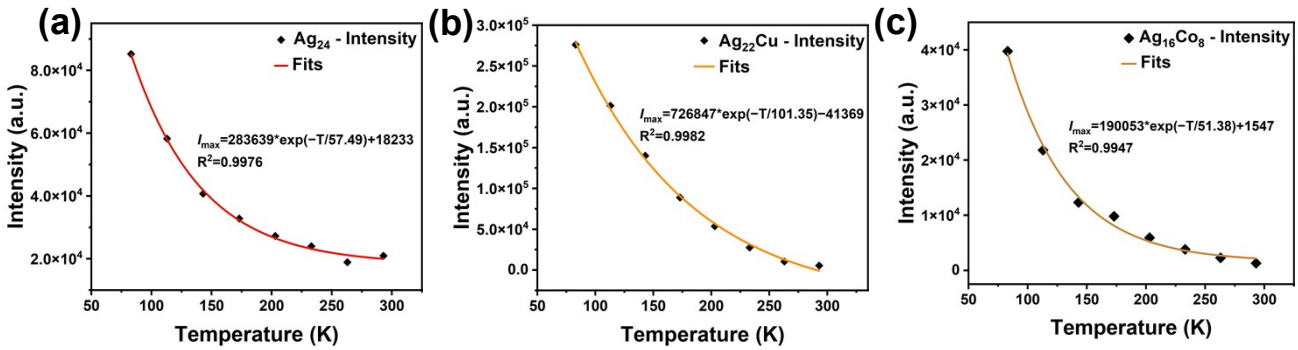

Fig. S16 Plots of maximum emission intensity of (a) **Ag_{24}**, (b) **$Ag_{22}Cu$**, and (c) **$Ag_{16}Co_8$** *versus* temperature in the range of 83 − 293 K.

Table S1. Crystal data and structure refinements for **Ag_{24}**, **$Ag_{22}Cu$** and **$Ag_{16}Co_8$**.

Compounds	**Ag_{24}**	**$Ag_{22}Cu$**	**$Ag_{16}Co_8$**
Empirical formula	$C_{195}H_{233}Ag_{24}ClO_{52.70}P_{12}S_{11}Si_{1.50}W_{15}$	$C_{195}H_{231.19}Ag_{22}ClCuF_{12}O_{34}P_{12}S_{11}Sb_2SiW_9$	$C_{250}Ag_{16}Co_8N_4O_{82}P_{16}S_6Si_2W_{18}$
M_r (g mol^{-1})	9568.48	8469.64	10621.26
Temperature/K	180(2)	180(2)	180(2)
Crystal system	Triclinic	monoclinic	Triclinic
Space group	*P-1*	*P2$_1$/n*	*P-1*
a (Å)	21.7876(2)	20.8060(3)	18.6002(2)
b (Å)	21.8079(2)	32.6834(5)	22.9769(3)
c (Å)	59.0524(4)	41.5251(8)	23.2397(3)
α (°)	86.9110(1)	90	67.8510(1)
β (°)	86.8350(1)	98.7177(2)	66.9270(1)
γ (°)	80.0060(1)	90	78.9240(1)
V/Å^3	27562.3(4)	27911.3(8)	8451.8(2)
Z	4	4	1
ρ_{calcd} (g cm^{-3})	2.306	2.016	2.087
μ mm^{-1}	8.116	5.681	7.561
F(000)	17826	15997.0	4848
Crystal size/mm^3	0.1 × 0.11 × 0.12	0.21 × 0.2 × 0.19	0.10 × 0.11 × 0.12
limiting indices	$-25 \le h \le 25$ $-25 \le k \le 25$ $-68 \le l \le 70$	$-24 \le h \le 24$ $-38 \le k \le 38$ $-47 \le l \le 49$	$-24 \le h \le 21$ $-28 \le k \le 29$ $-29 \le l \le 30$

no. of reflections collected	359565	236237	113256
no. of independent reflections	96956	49117	37761
restrains/parameters	17199/6311	4635/2453	55/1802
θ_{min} /θ_{max}	1.991 / 25.000	1.934 / 25.000	2.158 / 27.499
R_{int}	0.0797	0.0661	0.0445
GooF	1.219	1.028	1.021
R [$I > 2\sigma$]	R_1 = 0.1503	R_1 = 0.1165	R_1 = 0.0495
	wR_2 = 0.3287	wR_2 = 0.2989	wR_2 = 0.1216
R(all data)	R_1 = 0.1564	R_1 = 0.1655	R_1 = 0.0796
	wR_2 = 0.3312	wR_2 = 0.3435	wR_2 = 0.1383

$\boldsymbol{R_1 = \sum(|F_o| - |F_c||/\sum|F_o|, wR_2 = \{\sum[w(F^2_o - F^2_c)^2]/\sum[w(F^2_o)^2]\}^{1/2}}$.

Table S2. Selected bond distances (Å) for **Ag_{24}**.

W1	O1	1.908(1)	Ag3	Ag8	2.775(9)
W1	O2	1.903(1)	Ag3	Ag56	3.300(1)
W1	O3	1.895(1)	Ag3	S3	2.410(3)
W1	O4	1.895(1)	Ag3	S23	2.570(4)
W1	O14	1.897(1)	Ag5	Ag22	3.161(7)
W2	O2	1.900(1)	Ag5	Ag56	3.032(7)
W2	O7	1.899(1)	Ag5	S9	2.380(2)
W2	O8	1.892(1)	Ag5	S17	2.350(2)
W2	O9	1.893(1)	Ag8	Ag21	2.891(7)
W2	O16	1.896(1)	Ag8	Ag23	3.004(8)

W3	O1	1.906(1)	Ag8	Ag51	3.013(9)
W3	O6	1.897(1)	Ag8	Ag53	2.956(1)
W3	O7	1.900(1)	Ag8	Ag56	2.757(5)
W3	O11	1.896(1)	Ag8	Ag58	2.683(6)
W3	O15	1.892(1)	Ag8	O79	2.470(2)
W4	O4	1.896(1)	Ag8	O83	2.420(2)
W4	O5	1.890(4)	Ag11	S24	2.610(2)
W4	O9	1.901(1)	Ag11	P3	2.253(2)
W4	O10	1.902(1)	Ag11	O79	2.550(2)
W4	O17	1.894(1)	Ag13	Ag22	3.310(1)
W5	O3	1.897(9)	Ag13	Ag56	3.035(1)
W5	O10	1.905(9)	Ag13	S3	2.390(3)
W5	O11	1.896(1)	Ag13	S25	2.400(3)
W5	O12	1.900(1)	Ag14	S1	2.499(1)
W5	O18	1.898(1)	Ag14	P4	2.402(1)
W6	O5	1.899(1)	Ag14	O93	2.350(2)
W6	O6	1.898(1)	Ag16	S4	2.472(1)
W6	O8	1.896(1)	Ag16	P8	2.381(1)
W6	O12	1.897(1)	Ag16	O47	2.330(2)
W6	O13	1.893(1)	Ag19	Ag42	3.108(8)
O14	C275	1.600(4)	Ag19	S9	2.350(2)
Ag	S18	2.162(2)	Ag19	S19	2.360(2)
Ag	P5	2.510(2)	Ag21	S19	2.410(2)
Ag	O64	2.490(2)	Ag21	S21	2.317(1)
Ag1A	S26A	2.530(3)	Ag22	S16	2.522(1)
Ag1A	P9	2.878(2)	Ag22	S17	2.660(2)
Ag1A	O105	2.530(2)	Ag22	S25	2.620(3)
Ag2	Ag4	3.039(6)	Ag22	P10	2.396(1)
Ag2	Ag50	2.729(7)	Ag22	O99	2.410(2)

Ag2	S14	2.080(2)	Ag23	S5	2.330(2)
Ag2	S32	2.398(2)	Ag23	S21	2.314(1)
Ag2	O107	2.490(2)	Ag25	S11	2.490(4)
Ag4	Ag7	2.857(1)	Ag25	S13	2.360(4)
Ag4	Ag17	2.927(5)	Ag26	S1	2.446(1)
Ag4	Ag18	2.759(4)	Ag26	P23	2.383(1)
Ag4	Ag27	2.935(1)	Ag28	Ag41	3.270(9)
Ag4	Ag35	2.792(6)	Ag28	S4	2.386(1)
Ag4	Ag44	2.803(4)	Ag28	S24	2.500(2)
Ag4	Ag45	3.077(7)	Ag28	S24A	2.290(2)
Ag4	Ag50	2.725(4)	Ag31	Ag39	3.330(8)
Ag4	Ag57	2.998(1)	Ag31	S3	2.76(3)
Ag4	Ag61	2.853(2)	Ag31	S16	2.467(2)
Ag4	Cl2	2.406(1)	Ag31	P15	2.440(2)
Ag6	S10	2.450(1)	Ag31	O77	2.460(2)
Ag6	P12	2.389(1)	Ag32	S1	2.369(1)
Ag7	S15	2.250(7)	Ag32	S16	2.386(1)
Ag7	S31	2.480(4)	Ag32	O61	2.530(2)
Ag9	Ag30	3.257(7)	Ag39	Ag56	2.666(7)
Ag9	S26	2.485(2)	Ag39	S5	2.360(2)
Ag9	P21	2.450(2)	Ag39	S17	2.560(2)
Ag9	O54	2.500(2)	Ag39	O77	2.520(2)
Ag9A	S26A	2.530(3)	Ag40	S6	2.430(1)
Ag9A	P21	2.240(2)	Ag40	P6	2.367(1)
Ag9A	O54	2.400(2)	Ag41	S24	2.460(2)
Ag10	S8	2.502(1)	Ag41	P11	2.550(3)
Ag10	P13	2.405(1)	Ag41	O83	2.490(2)
Ag10	O76	2.330(2)	Ag42	S9	2.960(2)
Ag12	S10	2.476(1)	Ag42	S11	2.680(4)

Ag12	P20	2.363(1)	Ag42	S20	2.529(1)
Ag12	O50	2.350(2)	Ag42	P1	2.400(1)
Ag15	Ag34	3.085(7)	Ag42	O103	2.430(2)
Ag15	S28	2.341(2)	Ag43	S20	2.769(2)
Ag15	S30	2.390(2)	Ag43	P19	2.390(2)
Ag17	Ag20	3.132(6)	Ag43	O110	2.440(2)
Ag17	Ag50	2.989(6)	Ag47	S4	2.451(1)
Ag17	S14	2.490(2)	Ag47	P14	2.385(1)
Ag17	S28	2.396(2)	Ag48	Ag60	3.063(1)
Ag18	Ag27	2.702(1)	Ag48	S6	2.352(1)
Ag18	Ag35	2.882(6)	Ag48	S20	2.355(1)
Ag18	Ag44	2.718(5)	Ag48	O95	2.480(2)
Ag18	Ag45	2.989(7)	Ag49	S11	2.420(4)
Ag18	Ag50	2.766(5)	Ag49	S25	2.420(3)
Ag18	Ag61	2.980(2)	Ag51	S13	2.270(4)
Ag18	O54	2.380(2)	Ag51	S23	2.480(4)
Ag18	O104	2.600(2)	Ag52	S6	2.479(1)
Ag18	O105	2.440(2)	Ag52	P2	2.398(1)
Ag20	Ag29	2.748(2)	Ag52	O89	2.600(2)
Ag20	S22	2.549(1)	Ag53	Ag56	2.270(1)
Ag20	S31	2.510(4)	Ag53	O86	2.540(2)
Ag20	P17	2.406(1)	Ag53	O103	2.100(2)
Ag20	O90	2.410(2)	Ag56	Ag58	2.813(6)
Ag24	S8	2.450(1)	Ag56	O77	2.540(2)
Ag24	P7	2.394(1)	Ag56	O80	2.450(2)
Ag27	Ag55	3.280(2)	Ag56	O99	2.380(2)
Ag27	S27	2.470(4)	Ag58	O103	2.490(2)
Ag27	S29	2.550(5)	Ag58	O110	2.390(2)
Ag29	Ag50	3.090(1)	Ag60	S20	2.224(2)

Ag29	S27	2.640(4)	Ag60	P19	2.430(2)
Ag29	S31	2.220(4)	Ag60	O110	2.530(2)
Ag30	S10	2.386(1)	Ag62	S24A	2.540(2)
Ag30	S26	2.483(2)	Ag62	P3	2.785(2)
Ag30	S26A	2.270(3)	Ag62	O79	2.570(2)
Ag33	S26	2.593(1)	Ag54	O98	2.480(2)
Ag33	P9	2.326(1)	Ag55	S7	2.380(4)
Ag33	O105	2.510(2)	Ag55	S29	2.420(5)
Ag34	S18	2.507(1)	Ag57	S7	2.380(4)
Ag34	P16	2.397(1)	Ag57	S15	1.930(6)
Ag34	O58	2.430(2)	Ag59	S22	2.428(2)
Ag35	Ag45	3.303(8)	Ag59	S27	2.830(4)
Ag35	S2	2.470(2)	Ag59	P24	2.318(2)
Ag35	S30	2.448(2)	Ag59	O107	2.470(2)
Ag36	S8	2.360(1)	Ag61	O58	2.070(3)
Ag36	S22	2.377(1)	Ag61	O62	2.540(3)
Ag36	O84	2.500(2)	Ag46	S12	2.471(1)
Ag37	S18	2.713(2)	Ag46	P22	2.368(1)
Ag37	P5	2.384(2)	Ag50	Ag61	2.170(2)
Ag37	O64	2.420(2)	Ag50	O90	2.390(2)
Ag38	S12	2.416(1)	Ag50	O92	2.410(2)
Ag38	P18	2.351(1)	Ag50	O107	2.590(2)
Ag44	Ag50	2.758(6)	Ag54	S12	2.392(1)
Ag44	O58	2.450(2)	Ag54	S18	2.364(1)
Ag44	O64	2.420(2)	Si3	O67	1.610(2)
Ag45	S2	2.430(2)	Ag45	S32	2.350(2)

Table S3. BVS values for Si and W atoms of **Ag_{24}**.

W1	5.832	W28	6.161
W3	6.133	W32	5.874
W6	6.111	W39	6.059
W7	6.222	W40	6.106
W8	6.039	Si1	3.939

Table S4. Selected bond distances (Å) for **$Ag_{22}Cu$**.

W1	O1	1.711(2)	Ag1A	Ag2A	2.806(6)
W1	O4	2.001(1)	Ag1A	Ag3A	2.751(4)
W1	O6	1.932(2)	Ag1A	Ag4	2.753(4)
W1	O7	2.362(2)	Ag1A	O26	2.552(2)
W1	O9	1.879(1)	Ag1A	O29	2.380(2)
W1	O10	1.990(1)	Ag1A	O30	2.555(2)
W2	O3	1.735(2)	Ag1A	Ag2	3.370(8)
W2	O5	1.948(2)	Ag1A	Ag3	3.057(6)
W2	O6	1.938(2)	Ag2A	Ag3A	2.731(5)
W2	O7	2.321(1)	Ag2A	Ag4	2.744(4)
W2	O8	1.887(1)	Ag2A	O27	2.516(2)
W2	O13	1.939(2)	Ag2A	O31	2.598(2)
W3	O2	1.713(2)	Ag2A	O32	2.457(2)
W3	O4	1.893(1)	Ag2A	Ag1	2.835(8)
W3	O5	1.934(2)	Ag3A	Ag4	2.824(3)
W3	O7	2.335(1)	Ag3A	O33	2.521(2)
W3	O11	1.893(2)	Ag3A	O34	2.400(2)
W3	O12	1.978(2)	Ag3A	Ag1	3.097(7)
W4	O10	2.182(1)	Ag3A	Cu6A	3.044(9)

W4	O15	1.920(2)	Ag3A	Ag3	3.094(6)
W4	O16	1.725(2)	Ag1B	Ag2B	2.797(1)
W4	O17	1.840(2)	Ag1B	Ag3B	2.626(1)
W4	O26	2.272(2)	Ag1B	Ag4	2.695(8)
W4	O30	1.790(2)	Ag1B	O30	2.388(2)
W5	O9	2.055(1)	Ag1B	Ag38	3.277(9)
W5	O14	1.744(2)	Ag1B	Ag41	2.675(1)
W5	O15	1.980(2)	Ag2B	Ag3B	2.789(1)
W5	O25	1.835(2)	Ag2B	Ag4	2.780(8)
W5	O26	2.310(2)	Ag2B	O33	2.451(2)
W5	O29	1.753(2)	Ag2B	Ag39	2.758(1)
W6	O8	2.152(1)	Ag3B	Ag4	2.791(7)
W6	O23	1.930(2)	Ag3B	O29	2.531(2)
W6	O24	1.746(2)	Ag3B	O34	2.459(2)
W6	O25	1.849(2)	Ag3B	Ag3	2.202(9)
W6	O28	2.285(2)	Ag4	Ag39	2.928(7)
W6	O34	1.768(2)	Ag4	Ag41	2.865(7)
W7	O13	2.144(2)	Ag4	Ag1	2.813(7)
W7	O21	1.843(2)	Ag4	Cu6A	2.925(9)
W7	O22	1.733(1)	Ag4	Cl25	2.412(7)
W7	O23	1.940(2)	Ag4	Ag3	2.871(6)
W7	O28	2.256(2)	O14	Ag8A	2.460(2)
W7	O33	1.747(2)	O14	Ag8B	2.590(2)
W8	O12	2.147(2)	O18	Ag19	2.579(2)
W8	O19	1.900(2)	O20	Ag13	2.500(2)
W8	O20	1.753(2)	O22	Ag14	2.470(2)
W8	O21	1.859(2)	O23	Ag20	2.570(2)
W8	O27	2.269(2)	O29	Ag6	2.460(2)
W8	O32	1.797(2)	O30	Ag5A	2.476(2)

W9	O11	2.154(1)	O30	Ag5B	2.417(2)
W9	O17	1.840(2)	O31	Ag10	2.408(2)
W9	O18	1.741(2)	O32	Ag9A	2.413(2)
W9	O19	1.930(2)	O32	Ag9B	2.395(2)
W9	O27	2.288(2)	O33	Ag11	2.417(2)
W9	O31	1.750(2)	O34	Ag7	2.494(2)
Si1	O7	1.674(1)	Ag15	S4	2.407(1)
Si1	O26	1.610(2)	Ag15	P18	2.379(1)
Si1	O27	1.620(2)	P1A	Ag9A	2.370(3)
Si1	O28	1.632(2)	Ag20	S2	2.385(9)
Ag11	S2	2.500(1)	Ag20	S4	2.387(1)
Ag11	S10	2.758(1)	P1B	Ag9B	2.396(2)
Ag12	S3	2.358(9)	Ag39	S10	2.576(1)
Ag12	S11	2.349(1)	Ag39	S9B	2.746(1)
Ag13	S3	2.444(9)	P11	Ag11	2.396(8)
Ag14	S4	2.456(1)	P12	Ag7	2.395(9)
Ag18	S5	2.355(1)	Ag38	Ag41	3.342(8)
Ag19	S3	2.440(9)	Ag38	S6	2.314(2)
Ag41	S8	2.534(1)	Ag38	S8	2.443(1)
Ag41	S9B	2.187(1)	P13	Ag6	2.367(1)
Ag5B	P20	2.729(1)	P14	Ag14	2.374(8)
Ag5B	S5	2.845(2)	P15	Ag13	2.359(9)
Ag5B	S8	2.007(2)	P16	Ag19	2.384(9)
Ag6	S5	2.491(1)	P17	Ag35	2.376(9)
Ag6	S6	2.626(2)	S1	Ag8A	2.360(1)
Ag7	S2	2.542(8)	S1	Ag8B	2.536(1)
Ag7	S7	2.516(1)	S1	Ag18	2.370(1)
Ag8A	P21	2.406(2)	Ag5B	Ag38	2.469(1)
Ag8B	P21	2.382(2)	Ag5A	S5	2.380(1)

Ag9A	S11	2.654(1)	Ag5A	S8	2.816(1)
Ag9B	Ag39	2.950(8)	Ag5A	P20	2.364(1)
Ag9B	S11	2.520(1)	Ag10	S11	2.430(1)
Ag9B	S9B	2.841(8)	S1	Ag35	2.430(1)
Ag10	P19	2.385(1)	S1	C304	1.780(5)

Table S5. BVS values for Si and W atoms of **$Ag_{22}Cu$**.

W1	5.732	W6	6.151
W2	5.862	W7	6.330
W3	5.996	W8	6.081
W4	6.184	W9	6.270
W5	6.279	Si1	4.688

Table S6. Selected bond distances (Å) for **$Ag_{16}Co_8$**.

W1	O1	2.312(6)	P7	Ag3	2.337(4)
W1	O19	1.723(7)	W4	O24	1.840(7)
W1	O3	1.999(6)	W6	O20	1.995(6)
W1	O9	1.792(7)	W6	O2	2.009(6)
W1	O27	1.914(6)	W6	O13	1.720(6)
W1	O26	1.993(6)	W6	O29	2.381(6)
W4	O21	1.851(6)	W6	O23	1.843(6)
W4	O20	1.988(6)	W6	O26	1.833(6)
W4	O2	1.990(6)	W8	O3	1.853(6)
W4	O6	1.727(6)	W8	O37	1.729(7)
W4	O29	2.422(6)	W8	O8	1.930(6)
W8	O41	2.329(6)	W5	O12	1.839(6)

W8	O23	1.979(6)	W5	O41	2.384(6)
W8	O40	1.888(6)	W5	O32	2.002(6)
W9	O21	1.967(5)	W5	O25	1.846(6)
W9	O5	1.917(6)	W5	O40	1.978(7)
W9	O11	1.731(7)	W3	O18	1.714(7)
W9	O4	2.017(7)	W3	O4	1.849(7)
W9	O14	1.786(7)	W3	O8	1.946(6)
W9	O22	2.305(6)	W3	O41	2.327(6)
W5	O7	1.720(7)	O9	Ag3	2.356(7)
W3	O32	1.873(6)	Ag9	O15	2.569(7)
W3	O24	1.981(6)	Ag5	S1	2.423(3)
W7	O35	1.728(6)	Ag5	P1	2.354(3)
W7	O1	2.338(6)	Ag5	O14	2.452(7)
W7	O12	2.015(6)	Ag1	S2	2.404(3)
W7	O30	1.788(7)	Ag1	P5	2.375(4)
W7	O27	1.962(6)	Ag1	O35	2.557(7)
W7	O28	1.897(7)	Ag7	S3	2.308(1)
W2	O5	1.941(7)	Ag7	P7	2.455(8)
W2	O15	1.731(6)	Ag7	O9	2.460(1)
W2	O16	1.790(7)	Co1	O20	2.011(6)
W2	O22	2.365(6)	Co1	O2	2.359(6)
W2	O25	2.010(6)	Co1	O29	2.041(6)
W2	O28	1.915(7)	Co1	O42	2.023(7)
Ag2	S1	2.386(3)	Co1	O39	2.013(6)
Ag2	P2	2.368(3)	Co4	O1	2.291(6)
Ag4	S1	2.458(3)	Co4	O9	2.061(7)
Ag4	P8	2.361(3)	Co4	O10	2.031(7)
Ag4	O16	2.379(7)	Co4	O36	2.127(7)
Ag4	O17	2.482(7)	Co4	O30	2.060(6)

Ag6	S3	2.437(3)	Co4	O39	2.018(6)
Ag6	P6	2.359(3)	Co2	Co3	2.995(2)
Ag6	O30	2.315(7)	Co2	O42	2.022(6)
Ag8	Ag7	3.244(2)	Co2	O10	2.055(7)
Ag8	S3	2.369(3)	Co2	O14	2.068(7)
Ag8	P3	2.364(3)	Co2	O16	2.040(6)
Ag9	Ag1	3.157(1)	Co2	O17	2.111(7)
Ag9	P4	2.376(3)	Co2	O22	2.284(6)
Ag9	S2	2.405(3)	Co3	O34	2.106(8)
Co3	O42	2.129(7)	S3	Ag3	2.584(5)
Co3	O10	2.104(6)	Si	O1	1.629(6)
Co3	O38	2.083(7)	Si	O29	1.663(6)
Co3	O39	2.131(7)	Si	O41	1.658(6)
Co3	O31	2.084(7)	Si	O22	1.624(7)

Table S7. BVS values for Si, W, Co and O atoms of **$Ag_{16}Co_8$**.

W1	6.058	W8	6.072
W2	6.081	W9	6.065
W3	6.154	Co1	1.805
W4	5.999	Co2	2.091
W5	6.075	Co3	1.962
W6	6.054	Co4	2.059
W7	6.112	Si1	3.799
O10	1.117	O39	1.069
O42	1.093		

Table S8. Comparison of photothermal performance to the reported literature works.

Formula	Photothermal Conditions	Maximum Temperature (°C)	Heating Rate (°C s^{-1})	Ref
$[(SiW_9O_{34})@\mathbf{Ag_{24}}(^{i}PrS)_{11}(DPPP)_6Cl]_2(SiW_{12}O_{40})$	532 nm	133	8.86	**This work**
$[(SiW_9O_{34})@\mathbf{Ag_{22}Cu}(^{i}PrS)_{11}(DPPP)_6Cl](SbF_6)_2$	1 W cm^{-2}	183.9	12.26	
$\{\mathbf{Ag_{16}}(^{i}PrS)_6(DPPP)_8(CH_3COO)_4[\mathbf{Co_4}(OH)_3SiW_9O_{33}]_2\}(CH_3CN)_4(H_2O)_2$		150.7	10.05	
$[(Mo_7O_{25})(Mo_6O_{22})(MoO_4)@\mathbf{Ag_{72}}(TC4A)_7(^{t}BuPhS)_{26}$-$(CH_3CN)_9(H_2O)]\cdot 11CH_3CN\cdot CH_2Cl_2$;	450 nm	56	9.44	**[4]**
$\{[Cl_2@\mathbf{Ag_{32}}(TC4A)_4(tBuPhS)_8(PhCOO)_6(MeCN)_3]\cdot 4MeCN\}_n$.	0.3 W cm^{-2}	142	25.11	
$[\mathbf{Ag_{31-x}Cu_x}Br_2(FUR)_{20}(TPP)_{10}]^{3+}$ $(0\leq x\leqslant 8)$	1 W cm^{-2} 532 nm 660 nm 808 nm	122 102 100	–	**[5]**
$\{\mathbf{Ag_{14}}[(TC4A)_6(V_9O_{16})](CyS)_3\}$;	660 nm	194	115	**[6]**
$\{\mathbf{Ag_{43}}S[(TC4A)_2(V_4O_9)]_3(CyS)_9(PhCOO)_3Cl_3(SO_4)_4(DMF)_3\cdot 6DMF\}$.	0.9 W cm^{-2}	105	55.3	
$[(CrO_4)_6@\mathbf{Ag_{54}}Cl(TC_4A)_6(CyS)_{15}(OAc)_2\ (CH_3CN)_2]\cdot 3CH_3CN$;	808 nm	411	403	**[7]**
$[(CrO_4)Cl_3@\mathbf{Ag_{33}}(TC_4A)_4$-$(CyS)_{10}(OAc)_2(CH_3CN)_2]\cdot 4CH_3CN\cdot 2CH_2Cl_2$.	0.7 W cm^{-2}	150	134	
$([\mathbf{Ag_{18}}(Mo_2O_5PTC4A)_6(EtS)_6(Tos)_2]\cdot 2Ag(CH_3CN)_3\cdot 4CHCl_3$	808 nm 0.35 W cm^{-2} 0.25 W cm^{-2} 0.15 W cm^{-2}	360 295 188	84.3 68 41.25	**[8]**
$[W_{10}O_{32}@Ag_{48}(CyS)_{24}(NO_3)_{16}]\cdot 4NO_3$ (Cy = cyclohexyl) (**Ag48T**)	660 nm, 0.3 W cm−2 0.4 W cm−2 0.5 W cm−2	>650 ℃	79.94 134.36 161.92	**[9]**

References

1. Z. Wang, H.-F. Su, X.-P. Wang, Q.-Q. Zhao, C.-H. Tung, D. Sun and L.-S. Zheng, *Chemistry*, 2018, **24**, 1640-1650.
2. T. Minato, K. Suzuki, K. Kamata and N. Mizuno, *Chemistry*, 2014, **20**, 5946-5952.
3. N. E. Brese and M. O'Keeffe, *Acta Cryst*, 1991, **47**, 192-197.
4. Z. Wang, Y.-J. Zhu, O. Ahlstedt, K. Konstantinou, J. Akola, C.-H. Tung, F. Alkan and D. Sun, *Angew. Chem. Int. Ed*, 2024, **63**, e202314515.
5. L. Fang, W. Fan, G. Bian, R. Wang, Q. You, W. Gu, N. Xia, L. Liao, J. Li, H. Deng, N. Yan and Z. Wu, *Angew. Chem. Int. Ed*, 2023, **62**, e202305604.
6. Z. Wang, Y.-J. Zhu, B.-L. Han, Y.-Z. Li, C.-H. Tung and D. Sun, *Nat. Commun*, 2023, **14**, 5295.
7. Z. Wang, Y. Wang, T.-Y. Xu, L. Li, C. M. Aikens, Z.-Y. Gao, M. Azam, C.-H. Tung and D. Sun, *Angew. Chem. Int. Ed*, 2024, **n/a**, e202403464.
8. Z. Wang, L. Li, L. Feng, Z. Y. Gao, C. H. Tung, L. S. Zheng and D. Sun, *Angew. Chem. Int. Ed*, 2022, **61**, e202200823.
9. K. Sheng, Z. Wang, L. Li, Z.-Y. Gao, C.-H. Tung and D. Sun, *J. Am. Chem. Soc*, 2023, **145**, 10595-10603.